한국표면공학회지
Journal of the Korean Institute of Surface Engineering
Vol. 34, No. 5, Oct. 2001
<연구논문>

The Development of Cl-Plasma Etching Procedure for Si and SiO_2

Jong Woo Kim*, Mi Young Jung**, Sung Soo Choi** and Jin-Hyo Boo*

** Center for Advanced Plasma Surface Technology, Sungkyunkwan University, Suwon 440-746, Korea*
*** Department of Physics, Sunmoon University, Ahsan 336-840, Korea*

Abstract

Dry etching of Si wafer and SiO_2 layers was performed using He/Cl_2 mixture plasma by diode-type reactive ion etcher (RIE) system. For Si etching, the Cl molecules react with the Si molecules on the surface and become chemically stable, indicating that the reactants need energetic ion bombardment. During the ion assisted desorption, energetic ions would damage the photoresist (PR) and produce the bad etch Si-profile.

Moreover, we have examined the characteristics of the Cl-Si reaction system, and developed the new fabrication procedures with a Cl_2/He mixture for Si and SiO_2-etching. The developed novel fabrication procedure allows the RIE to be unexpensive and useful a Si deep etching system. Since the etch rate was proved to increase linearly with fHe and the selectivity of Si to SiO_2 etch rate was observed to be inversely proportional to fHe.

1. Introduction

Up to now, general silicon etching process uses fluorine and chlorine gas plasma[1-3]. Feature of etching process using chlorine gas has high aspect ratio etch profile, fabricate to use Si nanosize tip of field emission and nanosize structure[4]. There have been several reports on the results of Cl_2 plasma analysis by means of various techniques[1, 5, 6]. Generally feed gas of Cl_2 plasma used inexpensive Ar or He gas. Heavier Ar ion support to desorb reaction product but have influence on ion damage of etch mask pattern. Meyer et al. have investigated the influence of the mass of incident ion on the gas-surface chemistry by varying the incident ion for silicon-fluorine and silicon-chlorine system[7]. Especially, addition of He gas rater than Ar gas to chlorine gas would reduce the ion damage on the etch mask along with trench control due to its low physical ion damage[2, 7]. He ion is better small size than Ar ion, so RIE system using He gas used Si-deep etcher. The results of Si etching procedure using He/Cl_2 mixture plasma have already been reported[8].

Dry etching technique provides easier controllability of anisotropic etching than wet etching process and advantage of dry etching is able to pattern of microstructure on silicon, III-V materials. Especially, chlorine-based plasma or chlorine ion beam have been used to etch Si. Al metal

or III-V semiconductor materials including GaAs and AlGaAs[9]. Chlorine molecule is different chemical reaction at Si and Al etching on chlorine -based plasma system. Therefore, the purpose of this study is research for optimization of chlorine-base plasma system and application of fabrication nanosize Si tip and Si pillars as well as SiO_2 layers.

2. Experimental procedure

Dry etching of Si wafer and SiO_2 layer was performed using conventional reactive ion etching (RIE) system. The etching chamber was pumped down to 10^{-4} Torr using rotary and booster pump. RF power was fixed at 300 W for the whole procedure and the typical pressure of the chamber was maintained to be 200 mTorr. Cl_2 gas was selected as an etching gas and its flow rate was fixed at 58.6 sccm. He + Cl_2 gas mixture was utilized in order to minimize the trenches in the bottom corners in addition to reduction of physical ion damage on the etch mask layer, such as oxide, photoresist and electron beam resist layer. The flow rate was varied from 0 to 120 sccm for the purpose of investigating the influence of He flow rate on the etching procedure.

Prior to the dry etching, conventional sample cleaning procedure and thermal oxidation of Si wafer were performed. With this thermally grown oxide layer, we was able to obtain the etching characteristics of both Si and SiO_2 simultaneously. An etching window for Si layer was formed through a basic photolithography. That is, a part of the SiO_2 layer was completely removed in order to expose the Si surface. Finally, dry etching procedure was performed with the He / Cl_2 mixture gas and the ratio of He flow rate to that of Cl_2 was systematically varied from 0% to 67%.

The magnitude of etch depth of SiO_2 was measured by field emission scanning electron microscope (FE-SEM) and that of Si was measured step profile by an alpha step. More or less, error in the values of the etched thickness is inevitable when etched depth is very small. However, the data shows consistency when etch time is over 60 s as described in section 3. In order to test the experimental result, the micron size line pattern was generated using conventional photolithography on the thermally grown oxide in addition to the 500 nm dot pattern fabrication of 500 nm thickness resist on the thermally grown SiO_2 layer using electron beam lithography.

3. Results and Discussion

Fig. 1 represents the variation of the etched thickness of Si layer with respect to the etching time. He flow rate has been varied from 0 to 120 sccm while Cl_2 gas flow rate is fixed at 58.6 sccm. That is, the ratio of He gas flow to the total inlet gas (Cl_2 + He) has been varied from 0% to 67%. In this figure, each symbol (such as the solid square, circle, up triangle, down triangle, dia-

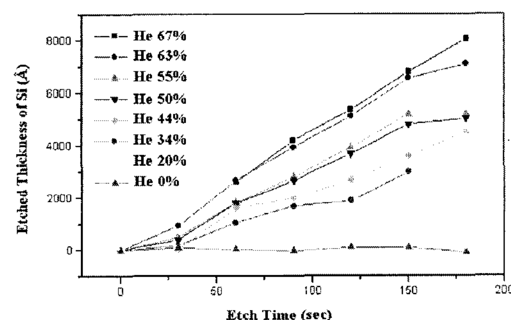

Fig. 1 Variation of the etched thickness of Si layer with respect to the etching tie for the various fractional He flow rate, f_{He}.

mond, +, ×, and *) represents the etched thickness when the fractional He flow rate, which is defined as (He flow rate) / (total inlet gas flow rate) and hereafter we will call it as fHe, is 67%, 63%, 55%, 50%, 44%, 34%, 20%, and 0%, respectively. The same symbols will be used throughout all the figures in this report.

As seen in Fig. 1, the etch depth increases linearly with etch time except two cases of f_{He} = 0% and 20%. In case of f_{He} = 0%, detectable etching was not observed. When f_{He} is low, the plasma state is unstable, which is thought to be a reason of the negligible etching. It is well established that even though molecular chlorine chemisorbed on Si, no etching is observable at room temperature with ion energy[10], and the processes of ion induced formation of $SiCi_4$(g), physical sputtering of $SiCl_x$(s), and the ion induced desorption of physisorbed $SiCi_4$(adsorbed) on the Si surface will be assisted by the energetic ions. These phenomena are reported for Ar/Cl_2 mixture gas[2, 7] but little data is available for He/Cl_2 mixture to the authors knowledge. In this experiment, when f_{He} is increased over 30% the plasma state becomes stable and the etch thickness reaches 7210 Å after etching of 180 s when f_{He} = 67%.

In order to see the influence of He flow more clearly, we have plotted the relation between Si etch rate (in the unit of Å/min) and f_{He} in Fig. 2. In this plot, we have disregarded the data obtained for f_{He} = 0%. Even though there are some fluctuations (this may be originated form the error in the thickness measurement), this plot shows good linearity between the two variables and proves the controllability of He/Cl_2 mixture plasma for the purpose of Si etching.

In Fig. 3, the etch rate versus etch time is presented for f_{He} > 40%. When the etch time (T_{etch}) is 30 s, the etch rate is relatively small compared to the other data points. This may be explained by the relatively low etch rate of SiO_2 layer using this He/Cl_2 mixture plasma. For example, the etch rate of SiO_2 for f_{He} = 44% is measured to be around 160 Å/min, and the full data will be described later. Thus, it will take a few seconds ($T_{native\ oxide}$) for the removal of native oxide on the Si surface and the actual Si etching time will be T_{etch}-$T_{native\ oxide}$. As the thickness of native oxide will be nearly the same for all the case, etch rate will be underestimated if the etching time is short such as 30 s. Therefore, if we correct this underestimation through more careful experiment having higher

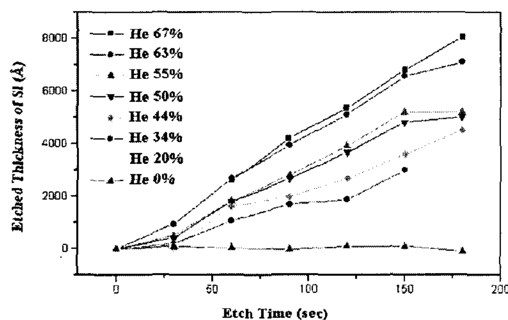

Fig. 2 Relation between Si etch rate (in the unit of Å/min) and the fractional He flow rate, f_{He}.

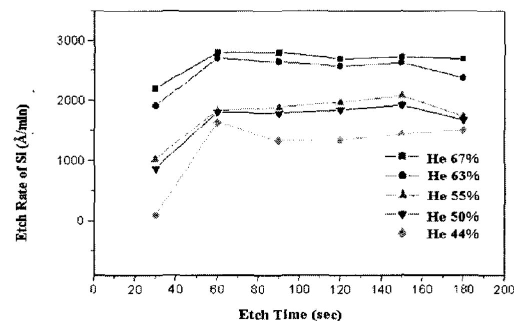

Fig. 3 Relation of the Si etch rate (in the unit of Å/min) versus etch time. The data is presented for f_{He} > 40%.

resolution, the curve will be expected to approach to an ideal one.

Now, we will describe the results of SiO_2 layer etching. Fig. 4 presents the variation of the etched thickness of SiO_2 layer with respect to the etching time. The etching condition and the symbols are the same as in Fig. 1 (from now on, the open symbols will be used instead of solid ones). Overall feature of the etching characteristics such as the linearity is nearly the same as the case of Si etching. One thing to be appointed is that the etch depth is vary thin compared with that of Si. For example, in the case of $f_{He} = 67\%$, the etched thickness of SiO_2 layer is around 450 Å, which is around 6% of the Si etch depth (7210 Å) obtained under the same etching condition. The relation between SiO_2 etch rate and f_{He} have been plotted in Fig. 5. The etch rate of SiO_2 seems to increase more steeply when f_{He} is higher than that of Si in the same region.

This fact indicates that more He flow rate may result in the higher SiO_2 etch rate and further experiment is to be done.

In Fig. 6, the etch rate of SiO_2 layer versus etch time is presented for $f_{He} > 40\%$ and the etch rate is regarded as nearly constant although fluctuation is large in some cases. As discussed above, the etch rate of SiO_2 layer is very low and proved to be less than 10% compared with that of Si etch result. The ratio of Si etch rate to SiO_2 etch rate is as selectivity plotted in Fig. 7. It seems that the selectivity is inversely proportional to f_{He}. For example, the ratio for $f_{He} = 67\%$, which suggests that the usage of He/Cl_2 mixture plasma can be developed into a good dry etching tool for both Si and SiO_2 layer having an easy controllability and selectivity.

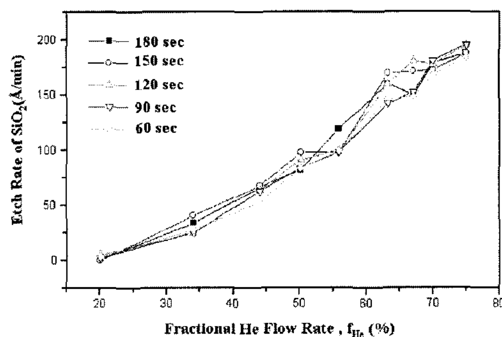

Fig. 5 Relation between SiO_2 etch rate (in the unit of Å/min) and the fractional He flow rate, f_{He}.

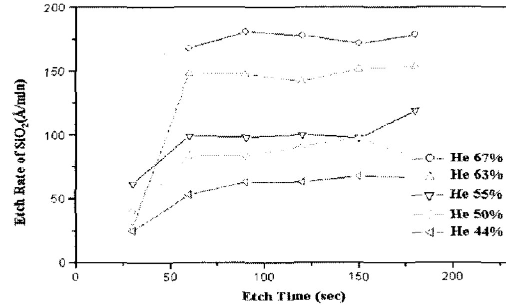

Fig. 6 Relation of the SiO_2 etch rate (in the unit of Å/min) versus etch time. The data is presented for $f_{He} > 40\%$.

Because the etch rate of Si wafer is almost the same as the cases of $f_{He} = 63\%$ and 67%, but that of SiO_2 layers for $f_{He} = 63\%$ is much smaller than that of $f_{He} = 67\%$, indicating that the optimization condition for Si and SiO_2 etching is better for $f_{He} = 63\%$ rather than for 67% due to consider thin oxidation layer. Therfore, we have chosen the etching procedure with the 63% He fractional flow rate to fabricate the Si deep trench and the nanosize Si pillar array. The micron size line pattern with conventional photolithography was patterned on the 600 nm thick oxide. A dot array pattern with 500 nm diameter on the 500 nm thick electron beam resist layer (ER) was also fabricated on the thermally grown oxide using

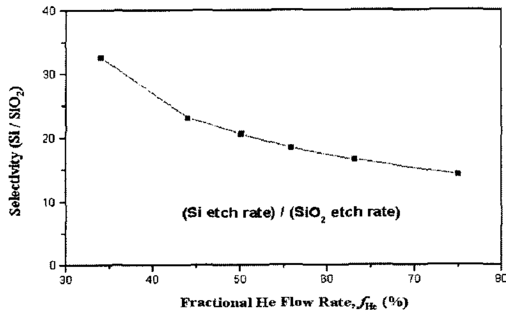

Fig. 7 Ratio of Si etch rate to SiO_2 etch rate, that is, selectivity. It seems that the ratio is inversely proportional to f_{He}.

electron beam lithography. In these experiments, the 500 nm SAL ER on the SiO_2 was remained in order to examine ion damage effect during dry etching. For the 10 μm deep Si trench fabrication, the thickness of the remained oxide was found to be ~ 100 nm (Fig. 8 (a)). On the other hand, the remaining 200 nm

PMMA ER was shown for 2.4 μm tall Si pillar array fabrication (Fig. 8 (b), (c)). The results were quite agreeable with the data (i.e. Figs. 1~6) for optimization etching procedure.

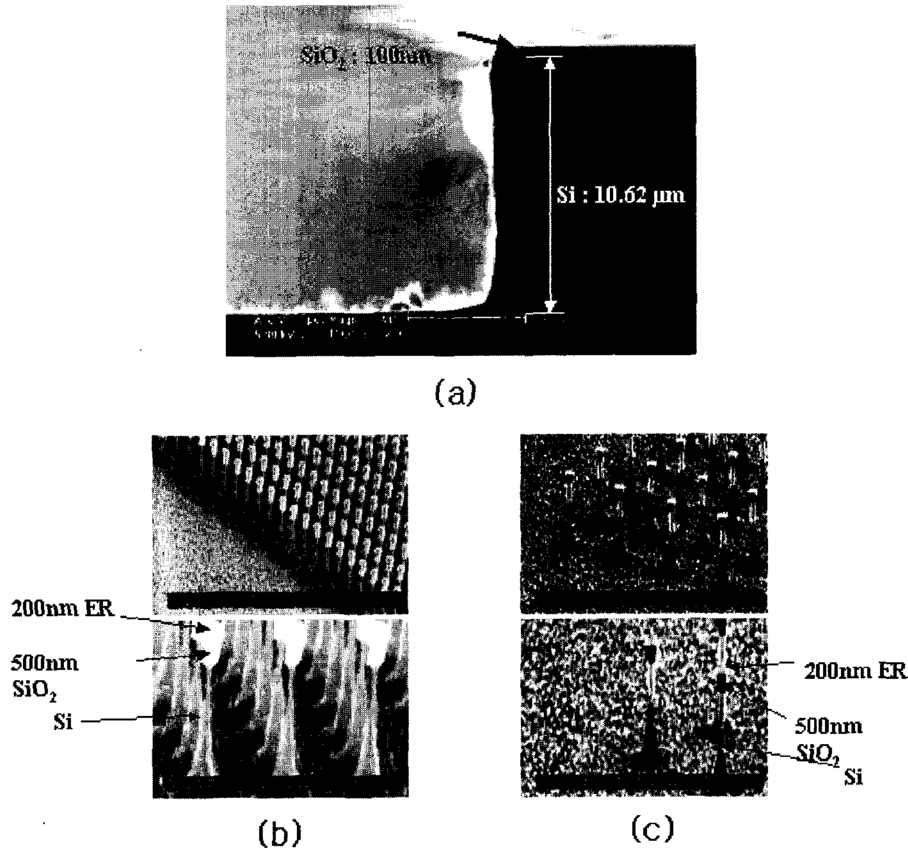

Fig. 8 (a) The SEM micrograph of a 10 μm deep Si sidewall with a trench on the bottom corner fabricated with 63% He fractional rate. The original 600 nm oxide etch mask was reduced down to 100 nm due to ion sputtering. (b) The SEM micrography for 2.4 μm tall Si-nanosize pillar array. Right figure shows the same SEM image of the left figure with more high magnification. (c) The remaining 200 nm PMMA on top of the oxide was seen. Right figure shows the same SEM image of the left figure with more high magnification. These micrographs reveal that the Si-nanosize pillar array can be fabricated using ER only.

4. Conclusions

The characteristics of the Si and SiO_2 dry etching using He/Cl_2 mixture plasma have been examined. The primary emphasis was placed on the influence of fractional He flow rate (f_{He}) on the etch rate and selectivity. Etching experiments were performed in a RIE system and the other parameters such as RF power and Cl_2 gas flow rate remained fixed through whole procedure. He flow rate was varied from 0 to 120 sccm. In case of low He flow rate, plasma state was rather unstable and the etch rate was measured to be negligible for both Si and SiO_2. As f_{He} increases over 30%, the plasma state becomes stable and the etch rate starts to increase. When $f_{He} > 60\%$, the relation between the etch depth and the etch time was observed to be nearly linear. Also, the etch rate was proved to increase linearly with f_{He} and the selectivity of Si to SiO_2 etch rate was observed to be inversely proportional to f_{He}. This preliminary study presents that the usage of He/Cl_2 mixture plasma can be developed into a good dry etching tool for both Si and SiO_2 layer having an easy controllability and selectivity.

The fabrication test procedures with 63% fractional flow rate were also applied. The fractional flow rate of 63% He was chosen due to its high Si etch rate and high oxide etch rate. The vertical side wall with 10 μm deep was successfully fabricated without trench on the bottom corner and the etch mask oxide layer still remained even with high oxide etch rate.

In addition, for the 2.4 μm tall Si pillar array fabrication, the remaining electron beam resistant layer with 200 nm thickness was seen. The tests reveal that He/Cl_2 mixture plasma can be utilized for etching even without an oxide mask.

References

1. B. Schwartz, H. Robbins, and J. Electrochem. Soc., **123** (1976) 1903-1905.
2. J.W. Coburn and H.F. Winters, J. Appl. Phys., **54** (1983) 5974-5975.
3. D.G. Schimmel, Soc., **126** (1979) 479-480.
4. P.B. Fischer and Y. Chou, Appl. Phys. Lett., **62** (1993) 1414-1415.
5. Helmut Crazzolara and Norbert Gellrich, J. Electrochem. soc., **137** (2) (1990. 2) 708-712.
6. H.B. Pogge, J.A. Bondur, and P.J. Burkhardt, J. Electrochem. soc., **130** (7) (1983. 7) 1983-1597.
7. U. Gerlach-Meyer, J.W. Coburn, and E. Kay, Surface Science., **103** (1981) 177-188.
8. G.C Schwartz and P.M. Schaible, J. Vac. Sci. Technol., **16** (1979) 410-412.
9. D.E. Ibbotson and D.L. Flamm, Solid State Technol., **31** (1988. 8) 77-78.
10. M.R. Rakhshandehroo, S.W. Pang,, J. Vac. Sci. Technol., **B14** (1996) 612.